Supplementary Information

S1. Synthesis of oleic acid capped Fe_3O_4 nanoparticles

The chemicals used to prepare the precursor solutionfor synthesis of nanoparticles are Ammonium iron (II) sulfate hexahydrate [$(NH_4)_2Fe(SO_4)_2 \cdot 6H_2O$] and Iron (III) sulphate hydrate [$Fe_2\ (SO_4)_3 \cdot xH_2O$] (purchased from *Sigma-Aldrich*). The oleic acid used for capping was purchased from *Alfa-Aesar*. All the chemicals were used as purchased. AR grade ethanol and de-ionised water were used as reagents.

Aqueous solutions of 0.2 mM $(NH_4)_2Fe(SO_4)_2 \cdot 6H_2O$ and 0.4 mM $Fe_2(SO_4)_3 \cdot xH_2O$ were mixed and stirred together for 30 min. Oleic acid (0.2 mM) was added into the above solution as a capping agent, followed by an aqueous solution of 3 mM NaOH. The pH of the solution was continuously monitored and maintained in the range of 11-12. The solution was constantly stirred for one hour at 80 ^oC, and subsequently cooled to room temperature. Then, the solution was filtered and a brownish precipitate was separated, which was washed several times with water and ethanol. The washed precipitate, consisting of nanoparticles was dispersed in ethanol.

S2. Characterization of Fe_3O_4 Nanoparticles

(a) Crystal structure

XRD profile of the as synthesised Fe_3O_4 nanoparticles is given in Figure S1. The peaks corresponding to (220), (311), (400), (422), (511) and (440) lattice planes were identified, which

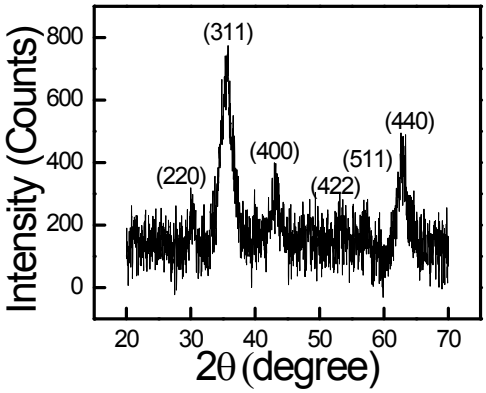

Fig.S1: *(a) X-Ray Diffraction pattern of as synthesized Fe_3O_4nanoparticles*

could be attributed to the face-centred cubic structure of magnetite, i.e. Fe_3O_4 (according to ICDD catalog no. 0-019-0629).

The crystallite size of the particles was calculated from the most prominent XRD peak (311) using the Debye Scherer equation:

$$D = \frac{0.9\lambda}{\beta cos\theta}$$

where, D is the average crystalline size, λ is the x-ray wavelength (1.54056 Å), θ is the Bragg diffraction angle and β is the FWHM. The crystallite size is found to be 4.7nm.

(b) Morphology and Particles Size

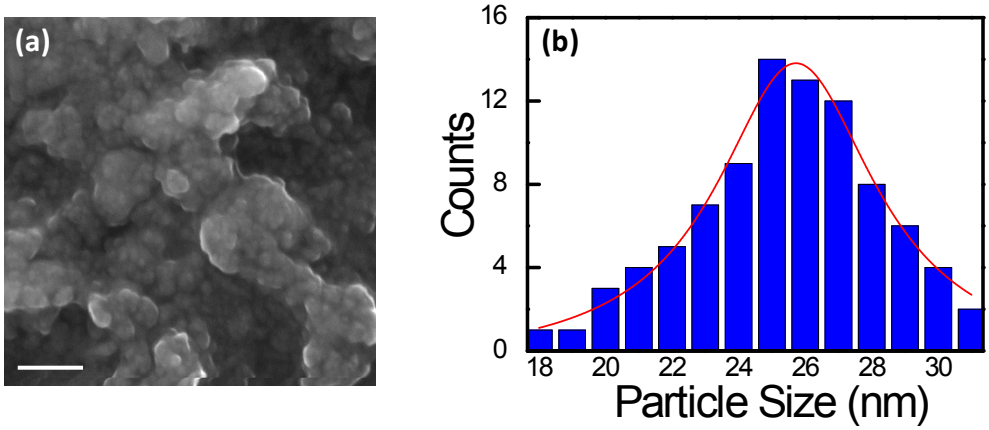

Fig. S2:*(a) FESEM image and (b) Particle size distribution curve of oleic acid capped Fe_3O_4 NPs. Scale bar in (a) is 200 μm*

FESEM image of the as prepared oleic acid capped Fe_3O_4 nanoparticles is given in Figure S2(a). The average particle shape is found to be spherical. The mean particle size is estimated to be around 25.7 nm, as shown in the size distribution curve of Figure S2(b).

S3. Polarising Optical Microscope (POM) Studies

Figure S3 depicts the POM images obtained for the FNLC composite filled in homeotropic cells. Images (a) and (c) show the homeotropically aligned nematic sol and gel states which transform to a planar aligned configuration, i.e. images (b) and (d) on application of an electric field (sine, 20V, 1kHz).

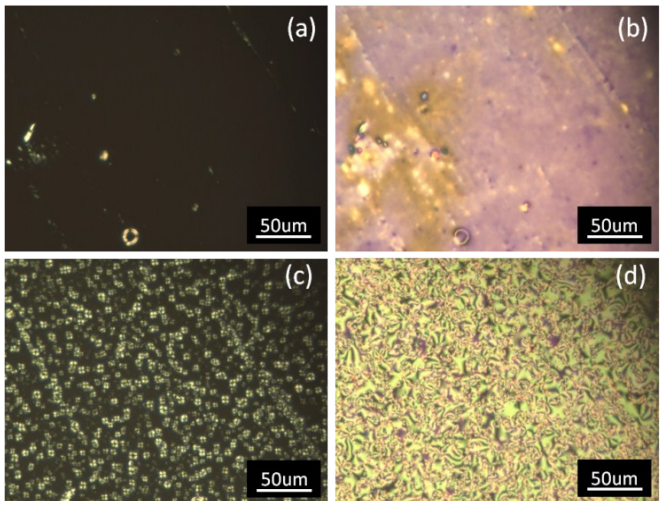

Fig. S3: *POM micrographs of nematic sol and nematic gel states of FNLC sample in their homeotropic (a & c) and planar (b & d) states respectively.*

S4. Gel morphology: FESEM

The high resolution FESEM images of the xerogel of FNLC-MNP composite obtained under high vacuum conditions, with operating voltage of 1.5 kV and 5 kV are shown in Figures S4 (a) & (b) respectively.

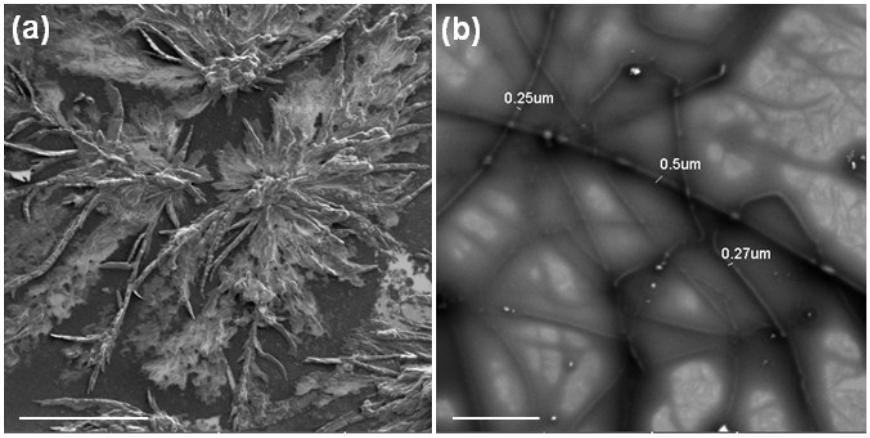

Fig.S4: *FESEM images of the xerogel of FNLC-MNP after the removal of liquid crystalline medium with DCM, followed by drying. Scale bar of (a) and (b) are 100μm and 5 μm respectively.*

The spherulitic structure of the gel network is clearly seen from Figure S4a, while the morphology of gel fibres obtained from the image at a higher magnification (Figure S4b) indicates variation in the thickness of gel fibres from 0.25 to 0.5μm.

S5. Internal magnetic moment of the nanoparticles:

Magnetic moment (μ) = M_s V, where M_s and V are the saturation magnetization and volume of the MNP respectively. For the present system,

M_s = 20 emu/cm^2 (see Figure 4a)

Particle size (d) = 26 nm

Hence, $\mu = (M_s \pi d^3)/6$

= 2.2 E-16 emu

S6. Zero field cooled (ZFC) and Field cooled (FC) magnetization studies:

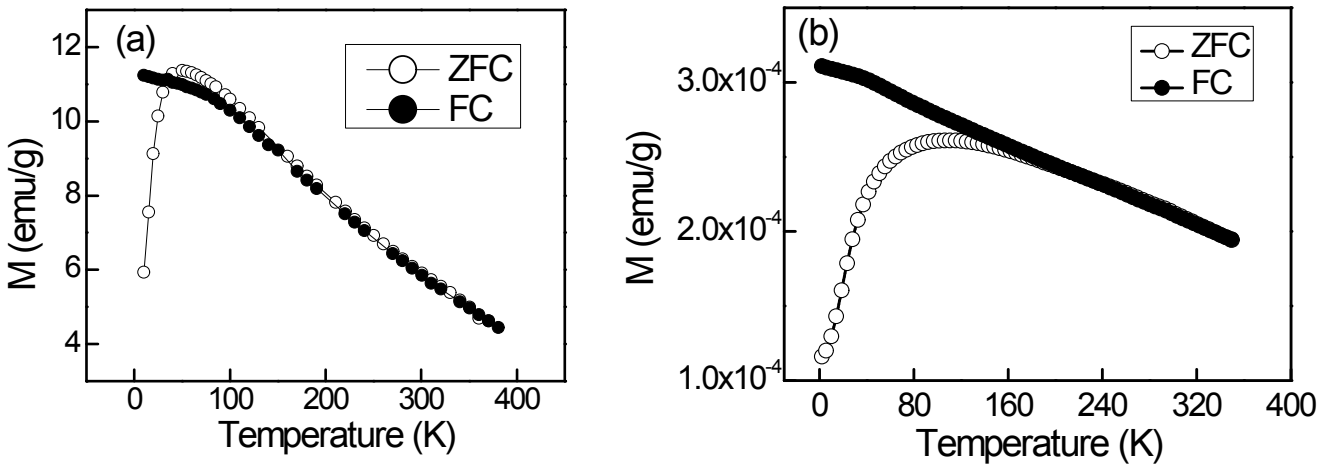

Fig. S5: *Thermal dependence of magnetization (M) under ZFC and FC conditions for the (a) as synthesized MNP and (b) FNLC-MNP composite with 1% MNP respectively.*

S7.Absorption studies of FNLC and FNLC-MNP samples:

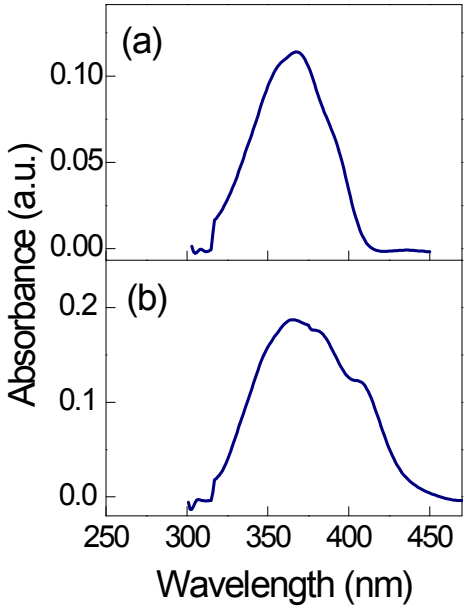

Fig. S6: *Absorption spectra of the (a) FNLC and (b) FNLC-MNP composites respectively.*

S8. Magnetic Freedericksz measurements:

The samples are filled in LC test cells (thickness ~ 25 μm) prepared using polyimide coated ITO plates. The cell is placed between the pole pieces of an electromagnet such that the magnetic

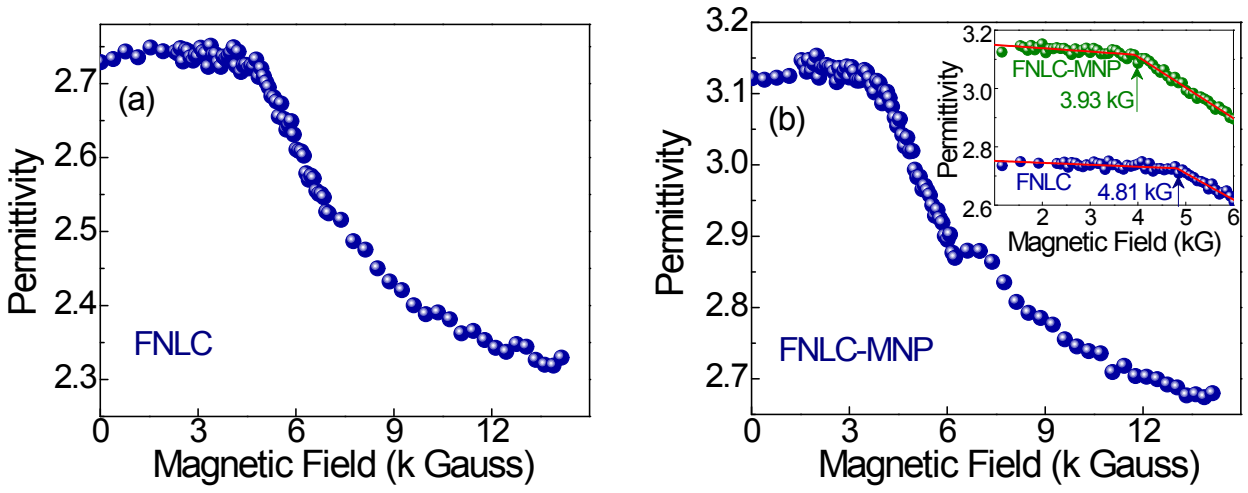

Fig. S7: *Magnetic field dependence of permittivity for the FNLC and FNLC-MNP composites at a temperature of 30°C.*

field lines are perpendicular to the substrate plane, due to the planar alignment, to begin with the LC directoris oriented normal to the magnetic field (B). As the 'B' value is increased, due to positive magnetic anisotropy, the molecules tend to orient towards the applied field. To probe the director orientation, permittivity (ε) of the sample is continuously measured using an LCR meter (*Agilent, E4980A*) with a small probing electric field of 0.1 V at a frequency of 1 kHz. The magnetic field is increased upto 1.5 T, which is large enough to orient the LC molecules homeotropically and the dependence of 'ε' on 'B' is shown in Figure S5.

Such a transition from planar to homeotropic configuration for a NLC is well known as the magnetic 'Freedericksz' transition. In the FNLC-MNP composite, threshold magnetic field required for the molecular reorientation decreases by 0.9 kG compared to FNLC (see inset of Figure S5b). This clearly indicates a coupling between applied 'B' and the internal magnetization (M) due to MNPs, which indirectly reorients the LC director at a much lower value of 'B'.

S9. PL enhancement as a function of MNP concentration

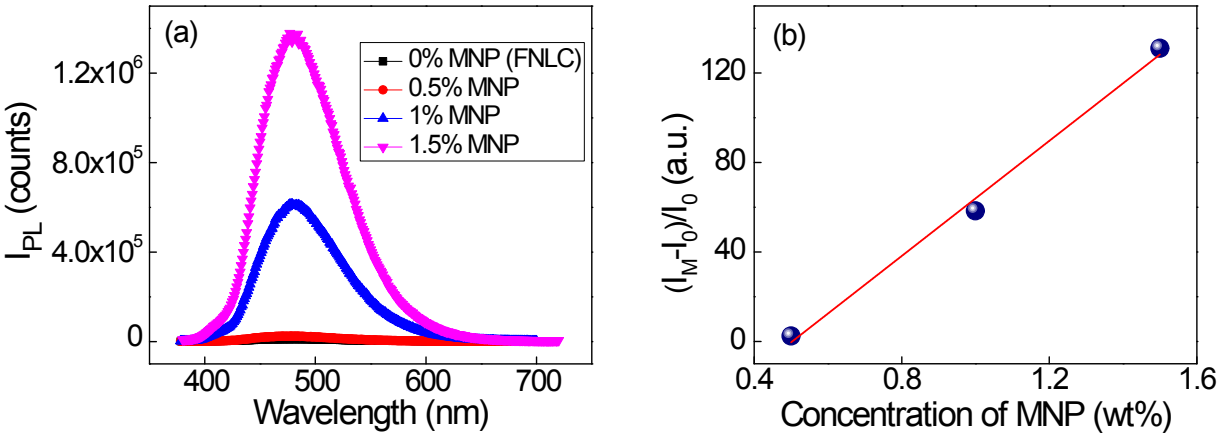

Fig. S8: *(a) PL spectra for the FNLC and various concentrations of MNP in the FNLC-MNP composite. (b) MNP% dependence of the relative PL enhancement, i.e.* $(I_M - I_0)/I_0$*, where* I_M and I_0 *are the PL intensities corresponding to the sample with and without MNP respectively.*

S10. XRD Studies:

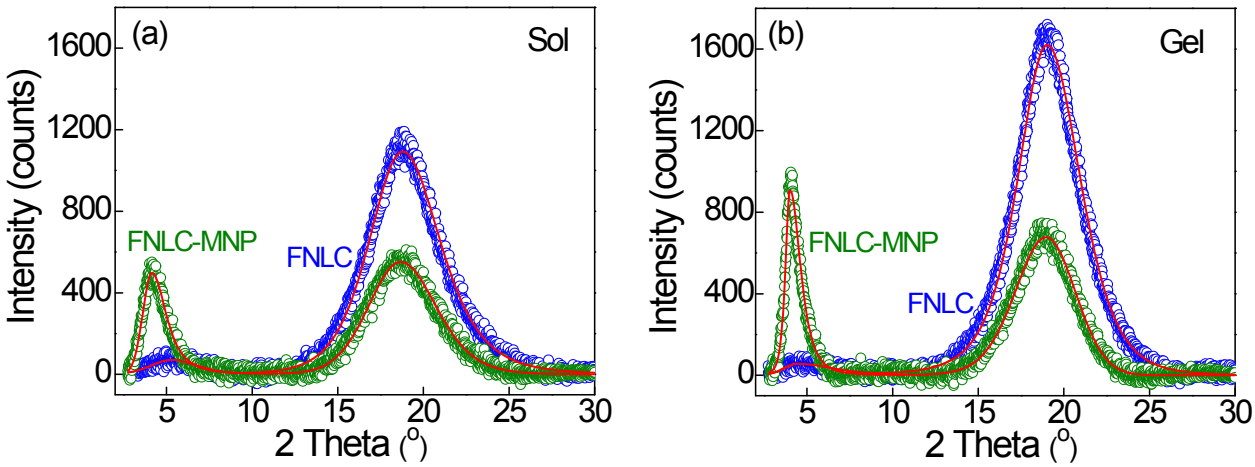

Fig. S9: *XRD profiles exhibiting the raw (open symbols) and fit (red line) data of both the composites in the (a) sol and (b) gel states.*

S11. PL measurements replacing NLC with organic solvent (THF):

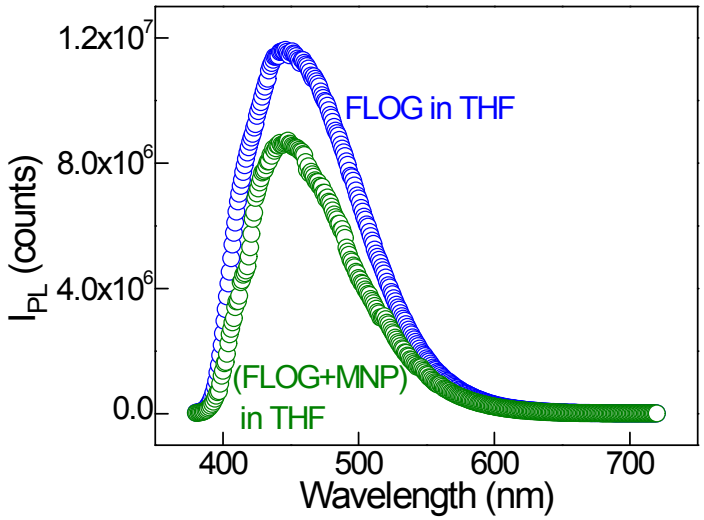

Fig. S10: *PL spectra of the FLOG in THF with and without MNP.*

S12. Photoluminescence switching:

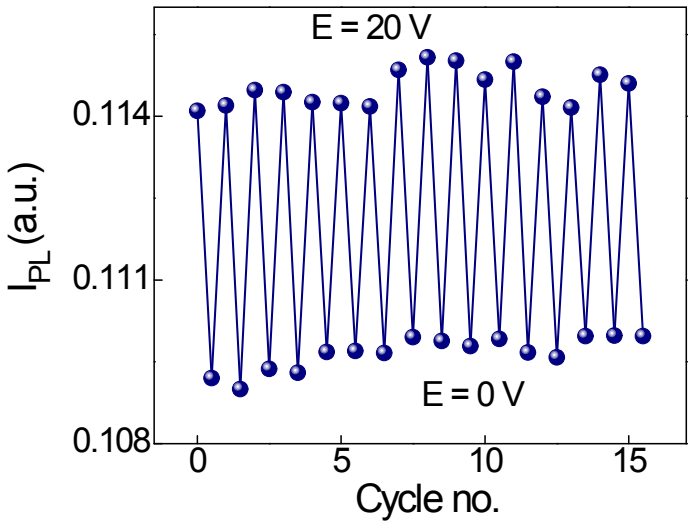

Fig. S11: *Switching of PL intensity between 'zero electric field' and 'with electric field' states in the FNLC-MNP sample demonstrating the repeatability of PL tuning.*